# Computer models of phase diagrams for ceramic systems. $TiO_2$-$SiO_2$-$Al_2O_3$ and $ZrO_2$-$SiO_2$-$Al_2O_3$

**Vasily LUTSYK** ▪ Institute of Physical Materials Science SB RAS and Buryat State University ▪ vluts@ipms.bscnet.ru
**Anna ZELENAYA** ▪ Institute of Physical Materials Science SB RAS ▪ zel_ann@mail.ru
**Aleksandr ZYRYANOV** ▪ Institute of Physical Materials Science SB RAS
**Edward NASRULIN** ▪ Institute of Physical Materials Science SB RAS

Érkezett: 2015. 12. 31. ▪ Received: 31. 12. 2015. ▪ http://dx.doi.org/10.14382/epitoanyag-jsbcm.2016.9

**Abstract**
The computer models and the analysis of structure for phase diagrams of ternary systems $TiO_2$-$SiO_2$-$Al_2O_3$ and $ZrO_2$-$SiO_2$-$Al_2O_3$ were performed. The calculation possibility of the crystallization paths and the diagrams of vertical and horizontal mass balances are demonstrated.
Keywords: computer model, phase diagrams, ceramic systems.

**Vasily LUTSYK**
Doct. Sci. (chemistry), Head of computer-aided materials design sector at the Institute of Physical Materials Science (Siberian Branch of the Russian Academy of Sciences). Research interests: Fluoride-chloride systems for the Generation IV molten salt reactor. Oxide and sulfide systems to elaborate the functional ceramic. Silicate systems for the advanced technologies of building materials. Fe-Ni-R-S (R=Cu, Co) systems to optimize the pyrometallurgy of Ni, Cu, Co. Bi-In-Se-Te, Pb-Sn-Se-Te to elaborate the thermoelectric materials. Liquid gap systems for the synthesis of refractory borides, silicides, intermetallics. Borate systems to grow the monocrystals. Metallic systems with the 3-phase reaction type changing for the titanium and zirconium alloys. Metallic systems for the lead-free solders.

**Anna ZELENAYA**
Cand. Sci. (phys.-math.), Senior Scientist at the Institute of Physical Materials Science (Siberian Branch of the Russian Academy of Sciences). Research interests: The elaboration of computer models of three-five phase diagram with different topology for microstructures design of heterogeneous material. An analysis of crystallization stages and identification the concentration fields with individual set of micro-constituents of phases assemblage. Simulation of phase diagram for ceramic, salt and metal systems.

**Aleksandr ZYRYANOV**
Scientist at the Institute of Physical Materials Science (Siberian Branch of the Russian Academy of Sciences). Research interests: Mathematical simulation, computer design, geometrical thermodynamics, multicomponent systems, phase diagrams, microstructure computation.

**Edward NASRULIN**
Scientist at the Institute of Physical Materials Science (Siberian Branch of the Russian Academy of Sciences). Research interests: Phase diagrams, microstructure, computer design of materials, software and models.

## 1. Introduction

Along with the experimental and thermodynamic investigation methods of phase diagrams of ceramic systems [1-6], one of the most effective methods to analyze them is to develop the 3D computer models, based on the description of phase regions boundaries [7-8].

The phase regions boundaries are reproduced and 3D models of phase diagrams are constructed on the basis of the scheme of mono- and invariant equilibria, which is compiled from data about the structure of binary systems and the proceeding invariant reactions. The elaborated models permit to calculate the isothermal sections and isopleths and to obtain the data about the crystallization stages for any part of phase diagrams.

We considered the phase diagrams of systems of $TiO_2$-$SiO_2$-$Al_2O_3$ and $ZrO_2$-$SiO_2$-$Al_2O_3$, as an example.

## 2. Model of $TiO_2$-$SiO_2$-$Al_2O_3$ T-x-y diagram

The phase diagram of system $TiO_2$-$SiO_2$-$Al_2O_3$ (A-B-C) is characterized by the presence of immiscibility surface from the side of binary system $SiO_2$-$TiO_2$ and two congruently melting compounds: $R_1 = 3Al_2O_3 \times 2SiO_2$ and $R_2 = Al_2O_3 \times TiO_2$ – from two other binary systems. The ternary system has one eutectic ($L_E \rightarrow TiO_2+SiO_2+R_2$) and two quasiperitectic ($L_{Q1}+Al_2O_3 \rightarrow R_1+R_2$, $L_{Q2}+R_1 \rightarrow SiO_2+R_2$) invariant transformations.

Using the coordinates of binary and ternary points as an initial data [1,9], the model of phase diagram containing an immiscibility surface was assembled (i), 5 liquidus surfaces ($q_A$, $q_B$, $q_C$, $q_{R1}$, $q_{R2}$), 17 ruled surfaces ($3i^r+14q^r$), 3 horizontal complexes at temperatures of invariant points ($h_E$, $h_{Q1}$, $h_{Q2}$) and 2 vertical planes, which are the degenerated ruled surfaces on the borders of the two-phase regions B+R2 and R1+R2 ($v_{BR2}$, $v_{R1R2}$) (*Fig. 1*).

The phase diagram includes 8 two-phase regions ($L_1+L_2$, L+A, L+B, L+C, L+R1, L+R2, B+R2, R1+R2) and 11 three-phase regions ($L_1+L_2+A$, L+A+B, L+A+R2, L+B+R1, L+B+R2, L+C+R1, L+C+R2, L+R1+R2, A+B+R2, B+R1+R2, C+R1+R2).

The crystallization path for the composition G(0.194; 0.198; 0.608) was calculated using the developed model (*Fig. 2.a*). Mass center G intersects four phase regions: L+R1, L+C+R1, L+R1+R2 and B+R1+R2, as well as two horizontal planes of four-phase regrouping of masses: $L^{Q1}+C \rightarrow R_1^{Q1}+R_2^{Q1}$ and $L^{Q2}+R_1 \rightarrow B^{Q2}+R_2^{Q2}$.

The melt composition moves along the ray $R_1G$ to the liquidus line $e_{CR1}Q_1$ while passing through two-phase region L+R1. Then mass center G falls into three-phase region L+C+R1 and shifts along the monovariant liquidus line $e_{CR1}Q_1$. After, it changes along liquidus line $Q_1Q_2$ at the intersection of three-phase region L+R1+R2 and two simplexes $R_1R_2Q_1$ and $R_1R_2Q_2$ of the horizontal complexes at the temperatures of the invariant points $Q_1$ and $Q_2$. Phase L is absent at the temperature below the plane $Q_2$ and the composition falls in the solid three-phase region B+R1+R2.

Crystallization stages are confirmed by the diagrams of vertical mass balances (*Fig. 2.b*), which allow to analyze the crystallization stages in the entire temperature range for the selected mass center. Given mass center G intersects the liquidus surface $q_{R1}$ and falls into the two-phase region L+R1, where the reaction of primary crystallization $L^1 \rightarrow R1^1$ takes place. Then the melt crosses the ruled surface $q^r_{R1C}$ on the border of three-phase region L+C+R1 with the proceeding of monovariant eutectic reaction $L^e \rightarrow C^e+R1^e$.

Further, the melt puts on the horizontal complex at the temperature of ternary quasiperitectic point $Q_1$ where the four-

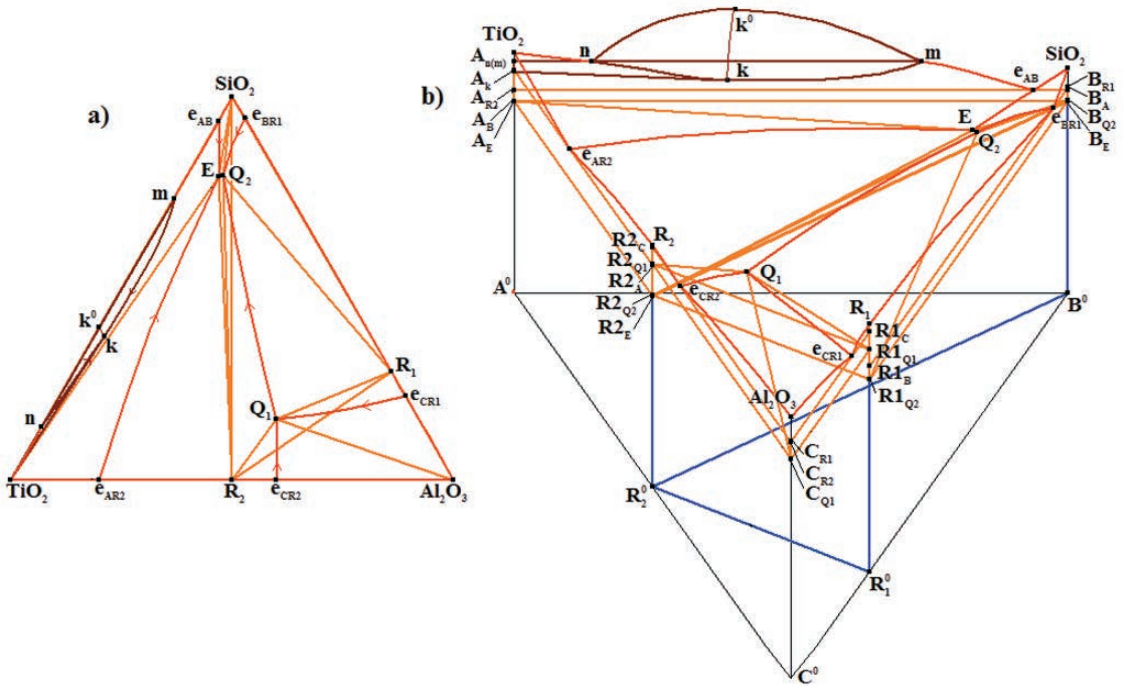


*Fig. 1. XY projection (a) and 3D model (b) of $TiO_2$-$SiO_2$-$Al_2O_3$ (A-B-C) T-x-y diagram*
*1. ábra $TiO_2$-$SiO_2$-$Al_2O_3$ (A-B-C) T-x-y diagram XY projekciója (a) és 3D modellje (b)*

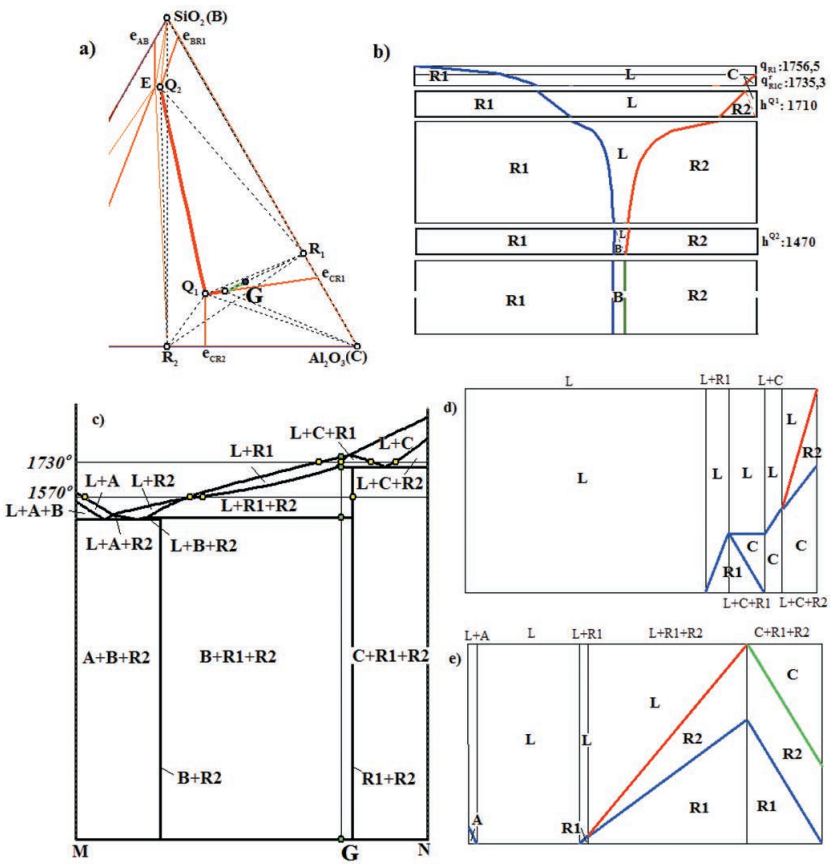


*Fig. 2. Crystallization path (a) and diagrams of mass balances:*
*vertical – for the composition G (b) and*
*horizontal (d,e) - for two isotherms of isopleth*
*M(0.194; 0.806; 0)-N(0.194; 0; 0.806)*
*2. ábra Az M(0.194; 0.806; 0)-N(0.194; 0; 0.806) izoplétán két izotermára vonatkozó*
*(a) kristályképződési út; (b) függőleges irányú tömegegyensúly diagram a G jelű összetételre;*
*(d,e) vízszintes irányú tömegegyensúly diagram a G jelű összetételre*

phase regrouping of masses $L^{Q1}+C \rightarrow R_1^{Q1}+R_2^{Q1}$ takes place. As the result the crystal C is fully expended during this reaction, but the crystals R1 and R2 are increased (therefore the crystal C is not included in the final set of micro-constituents).

Then there is the postperitectic secondary (eutectic) crystallization $L^{ep} \rightarrow R1^{ep}+R2^{ep}$ in the three-phase regions L+R1+R2. When mass center gets to the horizontal complex $h_{Q2}$ at the temperature of ternary quasiperitectic point $Q_1$, the invariant quasiperitectic reaction $L^{Q2}+R_1 \rightarrow B^{Q2}+R_2^{Q2}$ ends with the deficit of melt and below there are only crystals B, R1 and R2. As a result this field is characterized by the following set of micro-constituents: $R1^1$, $R1^e$, $R_1^{Q1}$, $R_2^{Q1}$, $R1^{ep}$, $R2^{ep}$, $B^{Q2}$, $R_2^{Q2}$.

The diagrams of horizontal mass balances at temperatures 1730° (*Fig. 2.d*) and 1570° (*Fig. 2.e*) were calculated on the isopleth M(0.194; 0.806; 0)-N(0.194; 0; 0.806) passing through the composition G (*Fig. 2.c*). Additionally, the isothermal sections were calculated at the same temperatures (*Fig. 3*).

## 3. Model for phase diagram of system $ZrO_2$-$SiO_2$-$Al_2O_3$

The phase diagram of the system $ZrO_2$-$SiO_2$-$Al_2O_3$ (A-B-C) has an immiscibility surface [1,10]. Compound $R_2 = ZrO_2 \times SiO_2$ decomposes without melt in the binary system $ZrO_2$-$SiO_2$ and the congruently melting compound $3Al_2O_3 \times 2SiO_2$ exists in

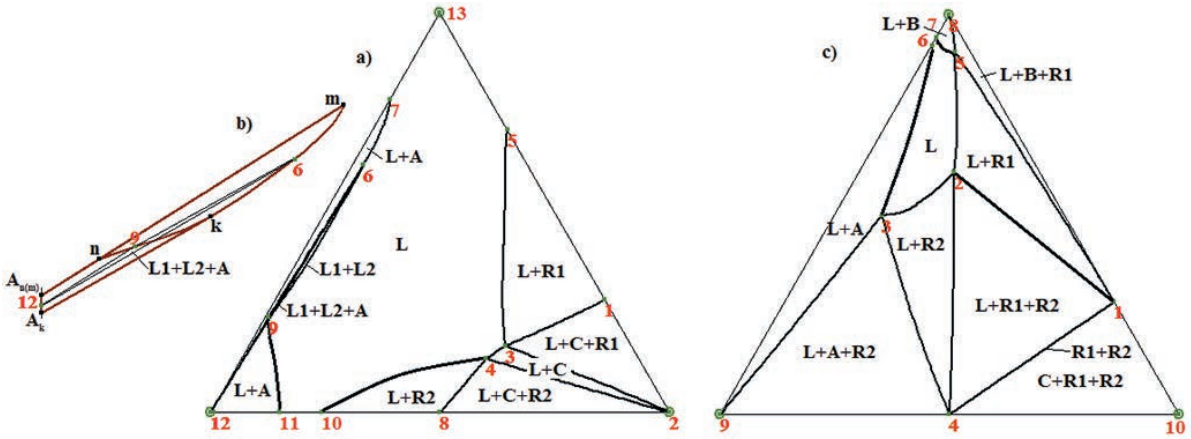


*Fig. 3. Isothermal sections at 1730° (a) and 1570° (c); an enlarged fragment of section of phase region L1+L2+A (6-9-12) in the perspective view (b)*
*3. ábra Izoterma metszetek 1730° (a) és 1570° (c) hőmérsékleten; a kinagyított részlet az L1+L2+A (6-9-12) fázismező perspektivikus képét ébrázolja (b)*

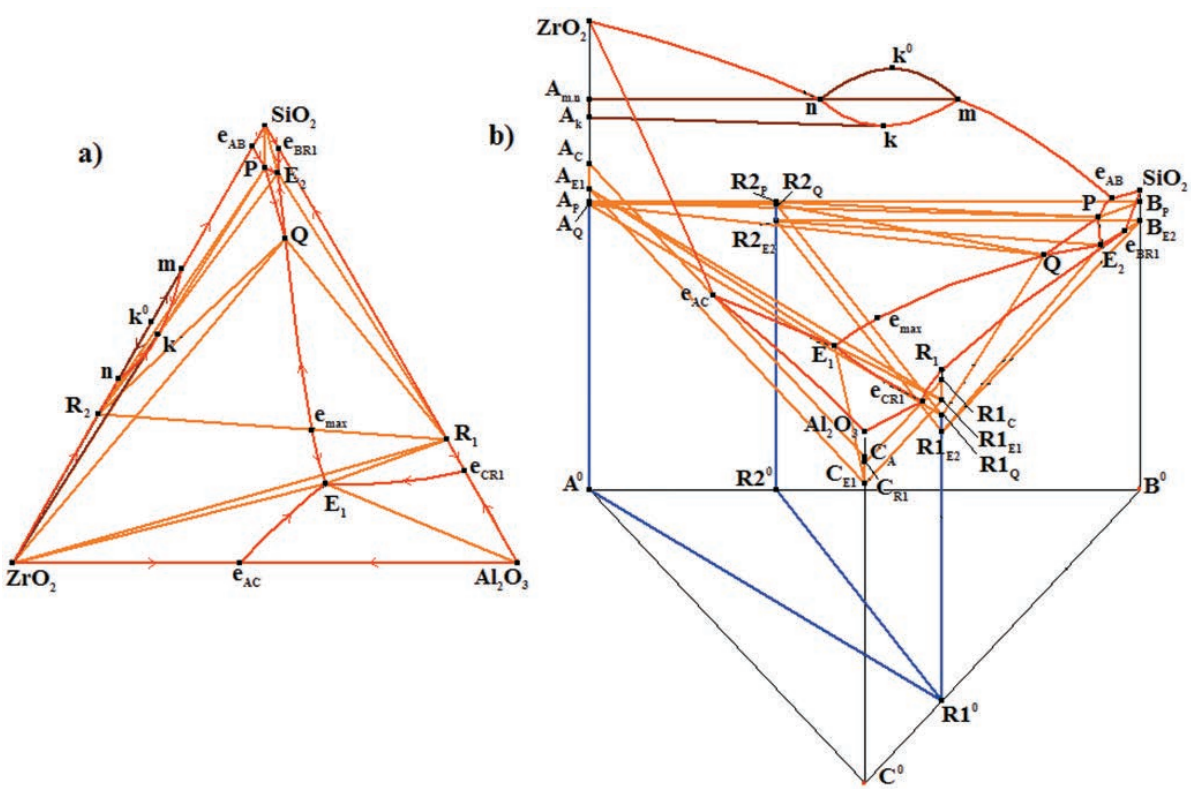


*Fig. 4. XY projection (a) and 3D model (b) of phase diagram of system $ZrO_2$-$SiO_2$-$Al2O_3$ (A-B-C)*
*4. ábra $ZrO_2$-$SiO_2$-$Al2O_3$ (A-B-C) fázisdiagram XY projekciója (a) és 3D modellje (b)*

the binary system $Al_2O_3$-$SiO_2$ [1]. There is a maximum point $e_{max}$ on monovariant liquidus line $QE_1$, which is the eutectic of quasi-binary section $R_1$-$R_2$.

There are the contradictions in the experimental data concerning the liquidus structure of system $ZrO_2$-$SiO_2$-$Al_2O_3$. Authors of [1,11] suggest the existence of four liquidus surfaces (excluding phase $ZrO_2 \times SiO_2$) and two invariant eutectic points. Authors of [2] show a fragment of phase diagram near the component $SiO_2$ with the liquidus field corresponding to the compound $ZrO_2 \times SiO_2$. The system includes four invariant points: two eutectic ($L_{E1} \rightarrow ZrO_2+Al_2O_3+R_1$, $E_2$: $L_{E2} \rightarrow SiO_2+R_1+R_2$), one quasiperitectic (Q: $L_Q+ZrO_2 \rightarrow R_1+R_2$) and one peritectic (P: $L_P+ZrO_2+SiO_2 \rightarrow R_2$) ones.

Because the compound $ZrO_2 \times SiO_2$ exists at the temperature higher than the invariant points, then it must correspond to the liquidus field, so we used variant [2] for the phase diagram assembling.

The model of phase diagram (*Fig. 4*) contains the immiscibility surface (i), 5 liquidus surfaces ($q_A$, $q_B$, $q_C$, $q_{R1}$, $q_{R2}$), 19 ruled surfaces ($3i^r+16q^r$), 4 horizontal complexes at the temperatures of invariant points ($h_{E1}$, $h_{E2}$, $h_Q$, $h_P$) and 2 vertical planes ($v_{AR1}$, $v_{AR2}$). Phase diagram includes 8 two-phase regions ($L_1+L_2$, L+A, L+B, L+C, L+R1, L+R2, A+R1, R1+R2) and 12 three-phase regions ($L_1+L_2+A$, L+A+B, L+A+C, L+A+R1, L+A+R2, L+B+R1, L+B+R2, L+C+R1, L+R1+R2, A+C+R1, A+R1+R2, B+R1+R2). A similar investigation for system $TiO_2$-$SiO_2$-$Al_2O_3$ can be carried using the obtained computer model.

## 4. Summary

Computer models of phase diagrams can produce the information about processes taking place in the investigated ceramic systems as well as can create a theoretical basis for experimental work. A detailed analysis of the structure of phase diagrams for systems $TiO_2$-$SiO_2$-$Al_2O_3$ and $ZrO_2$-$SiO_2$-$Al_2O_3$ can be used for the prediction of geometrical structure and the development of computer model of phase diagram for the quaternary system $TiO_2$-$ZrO_2$-$SiO_2$-$Al_2O_3$, which is applied in membrane technologies [12].

The comprehensive investigation of the phase diagrams of ceramic systems involves the analysis of crystallization processes in any part of the diagram. Forecast of microstructural constituents for the concentration fields of different dimensions (obtained by the projecting of all elements of the phase diagram into the Gibbs triangle) helps to plan and to reduce the volume of experimental study [13-16].

## 5. Acknowledgement

The work was partially supported by the Russian Foundation for Basic Research (projects 14-08-00453, 14-08-31468 and 15-43-04304).

### References

[1] Levin, E. M. – Robbins, C. R. – McMurdie, H. F. (1964): Phase diagrams for ceramists. *American. Ceramic Society*, Ohio, 600 p.

[2] Toropov, N. A. – Bazarkovsky, V. P. – Lapshin, V. V. et al (1972): Diagrams of Silicate Systems, vol. 3 Ternary Silicate Systems. *Nauka*, Leningrad, 448 p. (In Russian).

[3] Taylor, H. F. W. (1997): Cement Chemistry. *Thomas Telford*, London, 459 p.

[4] Lea, F. (1998): Lea's Chemistry of Cement and Concrete. *Elsevier Ltd*, London, 1057 p.

[5] Danek, V. (2006): Physico-chemical analysis of molten electrolytes. *Elsevier*, 464 p.

[6] Mao, H. – Hillert, M. – Selleby, M. – Sundman, B. (2006): Thermodynamic Assessment of the CaO–$Al_2O_3$–$SiO_2$ System. *Journal of the American Ceramic Society*. Vol. 89, No. 1, pp. 298-308. http://dx.doi.org/10.1111/j.1551-2916.2005.00698.x

[7] Lutsyk, V. – Zelenaya, A. (2013): Crystallization Paths and Microstructures in Ternary Oxide Systems with Stoichiometric Compounds. *Solid State Phenomena*. Vol. 200, pp. 73-78. http://dx.doi.org/10.4028/www.scientific.net/SSP.200.73

[8] Lutsyk, V. I. – Zelenaya, A. E. – Savinov, V. V. (2012): Phase Trajectories in CaO-$Al_2O_3$-$SiO_2$ Melts. *Crystallography Reports*. Vol. 57, No 7, pp. 71-74. http://dx.doi.org/10.1134/S1063774512070176

[9] Kirillova, S. A. – Almjashev, V. I. – Gusarov, V. V. (2011): Phase Relationships in the $SiO_2$–$TiO_2$ System. *Russian Journal of Inorganic Chemistry*. Vol. 56, No 9, pp. 1464–1471. http://dx.doi.org/10.1134/S0036023611090117

[10] Suzuki, M. – Sodeoka, S. – Inoue, T. – Structure. (2005): Control of Plasma Sprayed Zircon Coating by Substrate Preheating and Post Heat Treatment. *Materials Transactions*. Vol. 46, No. 3, pp. 669-674. https://www.jim.or.jp/journal/e/pdf3/46/03/669.pdf

[11] Ferrari, C. R. – Rodrigues, J. A. (2003): Microstructural features of alumina refractories with mullite-zirconia aggregates. *Boletin de la Sociedad Española De Cerámica y Vidrio*. Vol. 42, No 1, pp. 15-20. http://boletines.secv.es/upload/20090422111300.20034215.pdf

[12] Sintering of Ceramics – New Emerging Techniques (2012) Ed. by Dr. Arunachalam Lakshmanan. *InTech*, 610 p. http://dx.doi.org/10.5772/1882

[13] Lutsyk, V. I. – Vorob'eva, V. P. – Zelenaya, A. E. (2015): 3D Reference Book on the Oxide Systems Space Diagrams as a Tool for Data Mining. *Solid State Phenomena*. Vol. 230, pp. 51-54. http://dx.doi.org/10.4028/www.scientific.net/SSP.230.51

[14] Lutsyk, V. – Zelenaya, A. (2013): Crystallization paths in $SiO_2$-$Al_2O_3$-CaO system as a genotype of silicate materials. *Építőanyag - Journal of Silicate Based and Composite Materials*. Vol. 65, No 2, pp. 34-38. http://dx.doi.org/10.14382/epitoanyag-jsbcm.2013.7

[15] Lutsyk, V. I. – Vorob'eva, V. P. (2014): Algorithm for Topological Correction of Lists of Simplexes of Different Dimensions for Polyhedration of Multicomponent Systems. *Russian Journal of Inorganic Chemistry.* Vol. 59, No. 9, pp. 956-970. http://dx.doi.org/10.1134/S0036023614090125

[16] Lutsyk, V. I. – Vorob'eva, V. P. (2014): Search for Internal Diagonals in Polyhedration of Reciprocal Systems by the Algorithm for Topological Correction of Lists of Simplexes of Different Dimensions. *Russian Journal of Inorganic Chemistry.* Vol. 59, No. 10, pp. 1123-1137. http://dx.doi.org/10.1134/S0036023614100106

Ref.:
**Lutsyk**, Vasily– **Zelenaya**, Anna– **Zyryanov**, Aleksandr – **Nasrulin**, Edward: *Computer models of phase diagrams for ceramic systems. $TiO_2$-$SiO_2$-$Al_2O_3$ and $ZrO_2$-$SiO_2$-$Al_2O_3$*
Építőanyag – Journal of Silicate Based and Composite Materials, Vol. 68, No. 2 (2016), 52–55. p.
http://dx.doi.org/10.14382/epitoanyag-jsbcm.2016.9

**Kerámia rendszerek fázisdiagramjainak számítógépes modellezése. $TiO_2$-$SiO_2$-$Al_2O_3$ és $ZrO_2$-$SiO_2$-$Al_2O_3$**
A szerzők $TiO_2$-$SiO_2$-$Al_2O_3$ és $ZrO_2$-$SiO_2$-$Al_2O_3$ háromfázisú rendszerek fázisdiagramjainak számítógépes modellezését ismertetik. Bemutatják a kristályképződési utak számítási lehetőségeit és demonstrálják a függőleges és vízszintes irányú tömegegyensúly számítás lehetőségeit.
Kulcsszavak: számítógépes modell, fázisdiagram, kerámia rendszerek.